

1 Temporal dynamics of competition 2 between statistical learning and 3 episodic memory in intracranial 4 recordings of human visual cortex

5 **Brynn E. Sherman¹, Kathryn N. Graves¹, David M. Huberdeau¹, Imran H. Quraishi²,**
6 **Eiyemisi C. Damisah³, Nicholas B. Turk-Browne^{1,4}**

7 ¹Department of Psychology, Yale University; ²Department of Neurology, Yale University;

8 ³Department of Neurosurgery, Yale University; ⁴Wu Tsai Institute, Yale University

9

10 **Abstract** The function of long-term memory is not just to reminisce about the past, but also to make
11 predictions that help us behave appropriately and efficiently in the future. This predictive function of
12 memory provides a new perspective on the classic question from memory research of why we remember
13 some things but not others. If prediction is a key outcome of memory, then the extent to which an item
14 generates a prediction signifies that this information already exists in memory and need not be encoded.
15 We tested this principle using human intracranial EEG as a time-resolved method to quantify prediction in
16 visual cortex during a statistical learning task and link the strength of these predictions to subsequent
17 episodic memory behavior. Epilepsy patients of both sexes viewed rapid streams of scenes, some of
18 which contained regularities that allowed the category of the next scene to be predicted. We verified that
19 statistical learning occurred using neural frequency tagging and measured category prediction with
20 multivariate pattern analysis. Although neural prediction was robust overall, this was driven entirely by
21 items that were subsequently forgotten. Such interference provides a mechanism by which prediction can
22 regulate memory formation to prioritize encoding of information that could help learn new predictive
23 relationships.

24 **Significance Statement.** When faced with a new experience, we are rarely at a loss for what to do.
25 Rather, because many aspects of the world are stable over time, we rely upon past experiences to
26 generate expectations that guide behavior. Here we show that these expectations during a new
27 experience come at the expense of memory for that experience. From intracranial recordings of visual
28 cortex, we decoded what humans expected to see next in a series of photographs based on patterns of
29 neural activity. Photographs that generated strong neural expectations were more likely to be forgotten in
30 a later behavioral memory test. Prioritizing the storage of experiences that currently lead to weak
31 expectations could help improve these expectations in future encounters.

32

33 **Introduction**

34 Long-term memory has a limited capacity, and thus a major goal of psychology and neuroscience has been
35 to identify factors that determine which memories to store. Well-known factors include attention (*Aly and*
36 *Turk-Browne, 2017*), emotion (*Dolcos et al., 2017*), motivation (*Dickerson and Adcock, 2018*), stress (*Gold-*
37 *farb, 2019*), and sleep (*Cowan et al., 2021*). Here we propose a new factor that constrains long-term memory
38 formation.

39 Beyond reliving the past, a key function of memory is that it allows us to predict the future (*Schacter et al., 2012*). When faced with a new experience, we draw on related experiences from the past to know what is
40 likely to happen when and where (*De Brigard, 2014; Biderman et al., 2020*). This knowledge is the result
41 of statistical learning, which identifies patterns or regularities in the environment that repeat over time
42 (*Sherman et al., 2020; Endress and Johnson, 2021*) and form the basis of predictions (*De Lange et al., 2018*).
43 We hypothesize that the availability of these predictions during encoding affects whether a new memory is
44 formed. Namely, if one of the main objectives of long-term memory is to enable prediction, in the service of
45 adaptive behavior, experiences that already generate a prediction may not need to be encoded. In contrast,
46 experiences that yield uncertainty about what will happen next may be more important to store because
47 they can help learn over time what should have been expected. Note that this is distinct from whether
48 an experience being encoded was itself expected or unexpected, which also affects subsequent memory
49 (*Greve et al., 2017; Bein et al., 2021*); rather, we argue that the process of generating a prediction based on
50 the experience impedes its encoding.

51 We term this ability of an experience to generate a prediction its *predictive value*. There is some suggestive
52 evidence for predictive value as an encoding factor. In a statistical learning study with images presented
53 in temporal pairs, subsequent memory for the first item in a pair was impaired relative to unpaired control
54 items (*Sherman and Turk-Browne, 2020*). Because the first item in a pair was always followed by the second
55 item, it could have enabled a prediction of the second item and thus had predictive value.

56 However, this prior study was not able to link the predictive value of an item during encoding to subsequent
57 memory for that item for several reasons. One issue is that it was unclear whether the memory
58 impairment for the first item originated at the time of encoding or emerged in later stages such as consolidation
59 or retrieval. For example, the first item might have been encoded well, but when this item was probed
60 in the later memory test, its association with the second item interfered with recognition. The behavioral
61 experiments in the prior study were equivocal, as prediction was not measured during encoding. An fMRI
62 experiment provided some evidence of prediction during encoding — the category of the second item could
63 be decoded during the first — but the poor temporal resolution fMRI muddied this interpretation. The decoded
64 neural signals were recorded during or after the second item and shifted backward in time based
65 on assumptions about the hemodynamic lag. Methods with better temporal resolution could provide more
66 precise linking between neural signals and experimental events, allowing for more direct measurement of
67 predictions.

68 Another issue with the prior study is that it only examined the relationship between prediction and
69 encoding across participants. Average fMRI evidence for the category of second items during first items
70 was negatively associated with overall memory performance for first items. However, this could reflect a
71 generic individual difference — that participants who make more predictions tend to have worse memory
72 — rather than prediction having a mechanistic effect on encoding. According to the latter account, whether
73 a participant remembers or forgets a given item should depend on whether that item triggered a prediction
74 during its encoding. This requires testing for a relationship between prediction and encoding across items
75 within participant.

76 The present study addresses these issues to better establish predictive value as an encoding factor. We
77 combine intracranial EEG (iEEG) with multivariate pattern analysis, allowing us to measure neural predictions
78 in a time-resolved manner and link them to subsequent behavioral memory across trials. Epilepsy
79 patients viewed a rapid stream of scene photographs across blocks of a statistical learning task. The scenes
80 consisted of unique exemplars from various categories (e.g., beaches, mountains, waterfalls) that differed
81 by block. In the Random blocks, the order of “control” (condition X) categories from which the exemplars
82 were drawn was random. In the Structured blocks, the categories were paired such that exemplars from
83 “predictive” (condition A) categories were always followed by exemplars from “predictable” (condition B)
84 categories (**Figure 1A**). Patients were not informed of these conditions or the existence of category pairs,
85 which they learned incidentally through exposure (*Brady and Oliva, 2008*). The items from each category
86 were presented in sub-blocks that changed after four presentations (**Figure 1B**). After both blocks, patients
87 completed a recognition memory test for the exemplars from the stream.

88 To track statistical learning in the brain, we employed neural frequency tagging (*Batterink and Paller,*

Table 1. Patient Information.

ID	Age	Sex	nElec (vis)	Implant	Data Collected	Notes
1	19	F	203(21)	R G/S/D	2S, 2R	R2 mem data not usable (D)
2	26	F	163(59)	L G/S/D	2S, 2R	-
3	43	F	172(10)	Bi D	1S, 2R	-
4	61	F	136(0)	Bi D	1S, 1R	neural mem data not usable (T)
5	31	M	152(31)	L G/S/D	2S, 2R	R1 encoding data not usable (T)
6	69	F	92(7)	L D	2S, 2R	-
7	33	M	232(22)	Bi D	1S, 1R	-
8	31	F	192(20)	Bi D	2S, 2R	no mem data collected (C)
9	56	F	192(36)	Bi D	2S, 2R	R1 encoding data not usable (T)
10	53	M	148(0)	Bi D	2S, 2R	-

Description of patient participation. ID: patient participation number. Age: in years. Sex: M = Male, F = Female. nElec (vis): the total number of electrode contacts, followed by the number of visual electrode contacts. Implant: R = right-sided implant; L = left-sided implant; Bi = bilateral implant; G = grid; S = strip; D = depth. Data collected: the number of runs for each condition collected (S = Structured, R = Random). Notes: which runs (if any) were excluded from given analyses and why. D = patient distraction (e.g., a clinician coming in and disrupting testing); T = trigger issue (i.e., an error with the equipment such that we could not align individual trials to our neural signal); C = computer error (e.g., the computer crashed).

90 **2017; Choi et al., 2020; Henin et al., 2021.** We quantified the phase coherence of oscillations at the frequency of individual items (present in both Random and Structured blocks) and at half of that frequency reflecting groupings of two items (present only in Structured blocks with category pairs). To measure prediction during encoding, we used multivariate pattern similarity (Kok et al., 2014, 2017; Demarchi et al., 2019; Aitken et al., 2020). We first created a template pattern for each scene category based on the neural activity it evoked in visual contacts. We then quantified the expression of these categories during statistical learning, defining prediction as evidence for the second category in a pair evoked by items from the first category. In sum, by assessing iEEG signals during the rapid presentation of scenes, we measured the neural representations underlying statistical learning and prediction, and linked these online learning measures to offline memory, revealing how predictive value constrains memory encoding.

100 Materials and Methods

101 Participants

102 We tested 10 participants (7 female; age range: 19-69) who had been surgically implanted with intracranial 103 electrodes for seizure monitoring. Decisions on electrode placement were determined solely by the clinical 104 care team to optimize localization of seizure foci. Participants were recruited through the Yale Comprehensive 105 Epilepsy Center. Participants provided informed consent in a manner approved by the Yale University 106 Human Subjects Committee.

107 A summary of patient demographics, clinical details, and research participation can be found in **Table 1**. 108 Given electrode coverage and usable data, we retained 9 patients in the behavioral analyses, 8 patients in 109 the neural frequency tagging analyses, and 7 patients in the neural category evidence analyses.

110 iEEG recordings

111 EEG data were recorded on a NATUS NeuroWorks EEG recording system. Data were collected at a sampling 112 rate of 4096 Hz. Signals were referenced to an electrode chosen by the clinical team to minimize noise in 113 the recording. To synchronize EEG signals with the experimental task, a custom-configured DAQ was used 114 to convert signals from the research computer to 8-bit “triggers” that were inserted into a separate digital 115 channel.

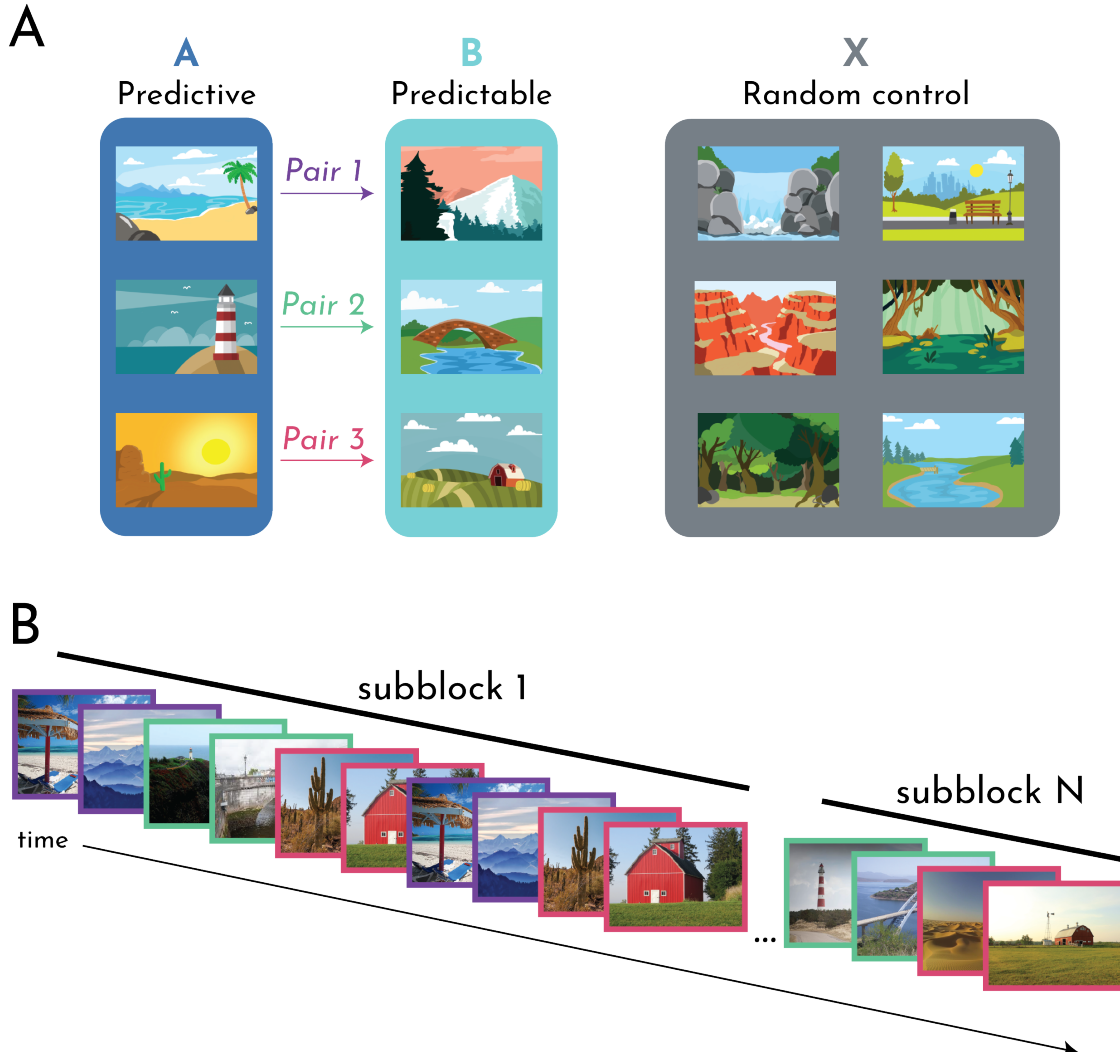


Figure 1. Task design. (A) Example scene category pairings for one participant. Three of 12 categories were assigned to condition A. Each A category was reliably followed by one of three other categories assigned to condition B to create pairs. The remaining six categories assigned to condition X were not paired. Participants viewed the A and B (Structured) and X (Random) categories in separate blocks of the task. (B) Example stimuli from the Structured block. Participants passively viewed a continuous stream of scenes. Each scene was shown for 267 ms, followed by an ISI of 267 ms with only a fixation cross on the screen. The stream was segmented into subblocks. The same exemplar of each category was presented four times per subblock, and new exemplars were introduced for the next subblock. For the Structured block, the category pairs remained consistent across subblocks. Category pairs are denoted by a colored frame, corresponding to the A-B pairs (and colored arrows) in subpanel A.

116 **iEEG preprocessing**

117 iEEG preprocessing was carried out in FieldTrip (*Oostenveld et al., 2011*). A notch filter was applied to
118 remove 60-Hz line noise. No re-referencing was applied, except for one patient, whose reference was in
119 visual cortex, resulting in a visual-evoked response in all electrodes; for this patient, we re-referenced the
120 data to a white matter contact in the left anterior cingulate cortex. Data were downsampled to 256 Hz and
121 segmented into trials using the triggers.

122 **Electrode selection**

123 Patients' electrode contact locations were identified using their post-operative CT and MRI scans. Recon-
124 structions were completed in BioImage Suite (*Papademetris et al., 2006*) and were subsequently regis-
125 tered to the patient's pre-operative MRI scan, resulting in contact locations projected into the patient's pre-
126 operative space. The resulting files were converted from the Bioimagesuite format (.MGRID) into native
127 space coordinates using FieldTrip functions. The coordinates were then used to create a region of interest
128 (ROI) in FSL (*Jenkinson et al., 2012*), with the coordinates of each contact occupying one voxel in the mask
129 (**Figure 2**).

130 For purposes of decoding scene categories, we were specifically interested in examining visually respon-
131 sive contacts. We defined visual cortex on the MNI T1 2mm standard brain by combining the Occipital Lobe
132 ROI from the MNI Structural Atlas and the following ROIs from the Harvard-Oxford Cortical Structural Atlas:
133 Inferior Temporal Gyrus (temporooccipital part), Lateral Occipital Cortex (superior division), Lateral Occipital
134 Cortex (inferior division), Intracalcarine Cortex, Cuneal Cortex, Parahippocampal Gyrus (posterior division),
135 Lingual Gyrus, Temporal Occipital Fusiform Cortex, Occipital Fusiform Gyrus, Supracalcarine Cortex, Occipi-
136 tal Pole. Each ROI was thresholded at 10% and then concatenated together to create a single mask of visual
137 cortex.

138 To identify which contacts to include in analyses on a per-patient basis, this standard space visual cortex
139 mask was transformed into each participant's native space. We registered each patient's pre-operative
140 anatomical scan to the MNI T1 2mm standard brain template using linear registration (FSL FLIRT (*Jenkinson*
141 *and Smith, 2001; Jenkinson et al., 2002*)) with 12 degrees of freedom. This registration was then inverted
142 and used to bring the visual cortex mask into each participant's native space.

143 In order to ensure that the visual cortex mask captured the anatomical areas we intended, we manually
144 assessed its overlap between the electrodes and made a few manual adjustments to the electrode defini-
145 tion. For example, due to noise in the registrations between post-operative and pre-operative space, as well
146 as from pre-operative space and standard space, some grid and strip contacts appeared slightly outside of
147 the brain, despite being on the surface of the patient's brain. Thus, contacts such as these were included as
148 "visual" even if they were slightly outside of the bounds of the mask. Additionally, due to the liberal thresh-
149 olds designed to capture broad visual regions, some portions of the parahippocampal gyrus area contained
150 the hippocampus. Contacts within mask boundaries but clearly in the hippocampus were excluded.

151 **Procedure**

152 Participants completed the experiment on a MacBook Pro laptop while seated in their hospital bed. The task
153 consisted of up to four runs: two runs of the Structured block and two runs of the Random block. We aimed
154 to collect all four runs from each patient, but required a minimum of one run per condition for subject
155 inclusion. Given that the order of structured vs. random information can impact learning (*Jungé et al.,*
156 *2007; Gebhart et al., 2009*), the run order was counterbalanced within and across participants (i.e., some
157 participants received Structured-Random-Random-Structured and others Random-Structured-Structured-
158 Random). Participants completed the runs across 1-3 testing sessions based on the amount of testing time
159 available between clinical care, family visits, and rest times.

160 Each run consisted of an encoding phase and a memory phase. During the encoding phase, participants
161 viewed a rapid stream of scene images, during which they were asked to passively view the scenes. Partici-
162 pants were told that their memory for the scenes would be tested in order to encourage them to pay close
163 attention. Each scene was presented for 267 ms, followed by a 267 ms inter-stimulus interval (ISI) period

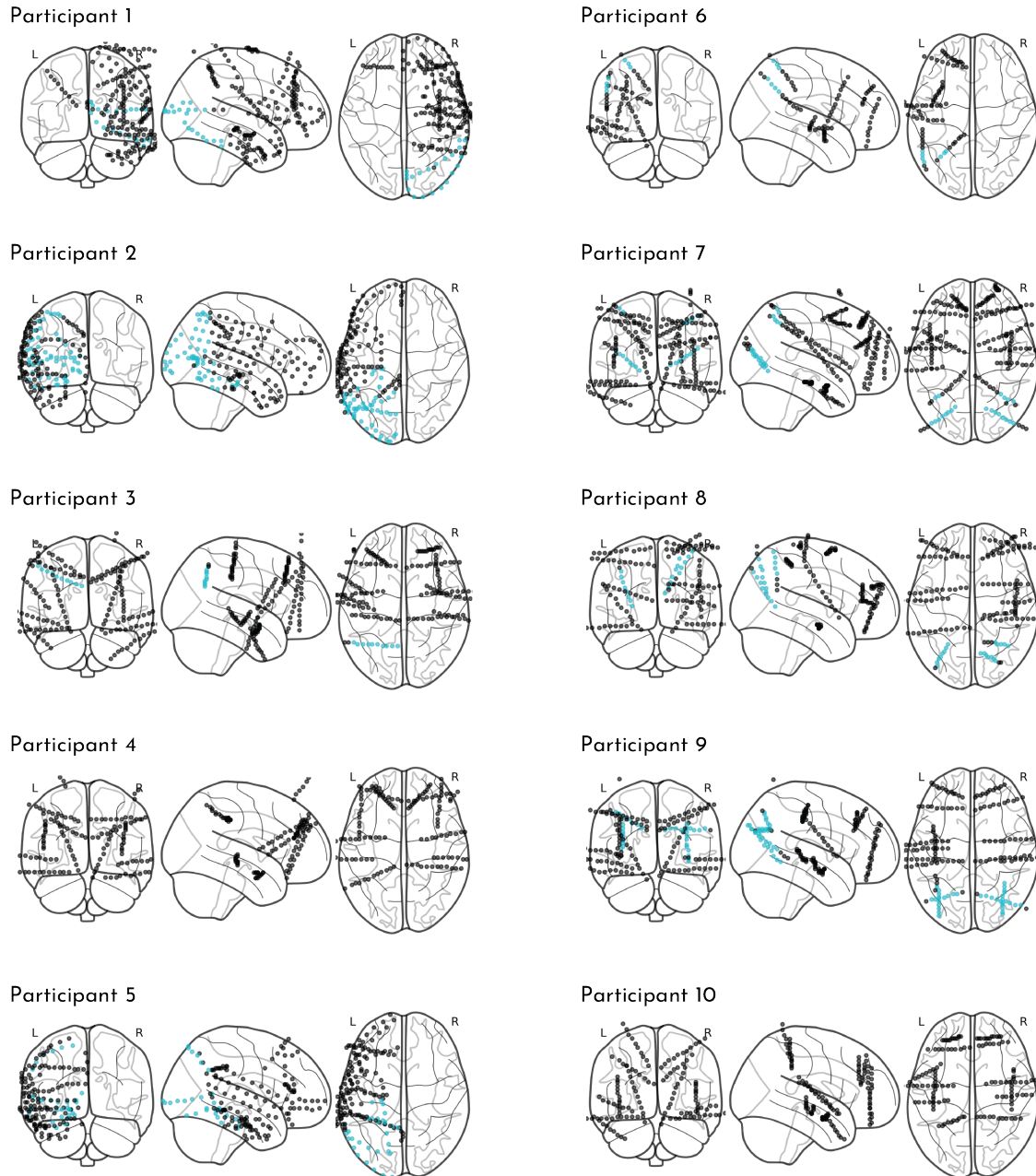


Figure 2. Electrode coverage. The contact locations on the grid, strip, and/or depth electrodes for each participant are plotted as circles in standard brain space. Contacts colored in blue were localized to the visual cortex mask.

164 during which a fixation cross appeared in the center of the screen. These short presentation times were cho-
165 sen to optimize the task for the frequency tagging analyses, which involves measuring neural entrainment
166 to stimuli.

167 Within each run, participants viewed a series of images from a set of six scene categories. There were
168 six categories in the Structured block, and six other categories in the Random block. In the Structured block,
169 the scenes categories were paired, such that images from one scene category (A) were always followed by
170 an image from another scene category (B). Thus, A scenes were *predictive* of the category of the upcoming
171 B scenes, or stated another way, the category of B scenes was *predictable* given the preceding A scenes.
172 No scene pairs were allowed to repeat back-to-back in the sequence. In the Random block, all six scene
173 categories (X) could be preceded or followed by any other scene category, making them neither predictive
174 nor predictable. No individual scene categories were allowed to repeat back-to-back.

175 In total, participants viewed 16 exemplars from each category within each run. To assist patients with
176 remembering these briefly presented images, each individual exemplar was shown four times within a run.
177 Thus, each run was comprised of 16 “subblocks” during which the same set of six exemplar images was
178 repeated four times (384 trials total). Within each subblock, the order of the pairs/images was randomized,
179 with the constraints described above of no back-to-back repetitions. The individual exemplars changed after
180 each subblock, but the category relations were held constant in the Structured block. Participants were not
181 informed of these category pairings, and thus had to acquire them through exposure.

182 At the end of each run, participants completed a memory test. Participants were presented with all
183 96 unique images from the encoding phase, intermixed with 24 novel foils from the same categories (4
184 foils/category). Participants first had to indicate whether the image was old, meaning it was just presented
185 in that run’s encoding phase, or new, meaning that they had not seen that image at all during the experiment.
186 Following their old/new judgment, participants were asked to indicate their confidence in their response, on
187 a scale of 1 (very unsure) to 4 (very sure). Participants had up to 6 s to make each old/new and confidence
188 judgment.

189 **Frequency tagging analyses**

190 We conducted a phase coherence analysis to identify electrode contacts that entrained to image and pair
191 frequencies (Henin *et al.*, 2021). For both Structured and Random blocks, the raw signals were concatenated
192 across runs (if more than one per block type) and then segmented into subblocks comprising 24 trials with
193 the four repetitions per exemplar. We then converted the raw signals for each subblock into the frequency
194 domain via fast Fourier transform and computed the phase coherence across subblocks for each electrode
195 using the formula $R^2 = [\sum^N \cos\phi]^2 + [\sum^N \sin\phi]^2$. Notably, by computing phase coherence between subblocks,
196 we collapsed over the contribution of individual exemplars that repeated within subblock. In other words,
197 entrainment in this analysis was driven by phase-locking that generalized across exemplars. Phase coher-
198 ence was computed separately for each contact in the visual cortex mask, and we then averaged across
199 contacts within participant. We focused on phase coherence at the frequency of image presentation (534
200 ms/image; 1.87 Hz) and pair presentation (1.07 s/pair; 0.93 Hz).

201 **Category evidence analyses**

202 We employed a multivariate pattern similarity approach to assess the timecourse of category responses.
203 We identified patterns of multivariate activity associated with each category across contacts, frequencies,
204 and time. These category patterns, or “templates”, were defined during the memory phase of the dataset.
205 This was important because the order of categories was random during the memory phase, allowing for
206 an independent assessment of each category across condition regardless of any pairings. We then used
207 these templates to examine category-specific evoked responses during the encoding phase, to assess the
208 presence and timing of category evidence (e.g., for the on-screen category or the upcoming category). The
209 following subsections explain this approach in detail.

210 *Frequency decomposition*

211 We employed a Morlet Wavelet approach to decompose raw signals into time-frequency information (**Figure 3A**). We convolved our data with a Complex Morlet Wavelet (cycles = 4) at each of 50 logarithmically
212 spaced frequencies between 2 and 100 Hz to extract the power timecourse at each of these 50 frequencies. This analysis was done separately for each encoding and memory phase of each run, and the data
213 were z-scored across time within each frequency and contact. This procedure was applied across the un-
214 segemented timecourses; we then subsequently carved into trials using the triggers, yielding a vector of
215 frequency and contact information at each timepoint within a trial.

216 Subsequent analyses required that each trial have the same number of timepoints. However, memory
217 trials were variable lengths, as participants had up to 6 s to respond. There was also slight variability in the
218 encoding trials (most trials were 138 samples long, but some were 136 or 137 samples). To account for this,
219 we considered only the first 138 samples of each memory trial and treated each encoding trial as having
220 138 samples (interpolating missing timepoints by averaging the last sample of the trial with the first sample
221 of the next trial).

222 *Feature selection*

223 We aimed to identify the set of timepoints that produced the best category discrimination. We reasoned
224 that time within a trial would be an important contributor to variance in discriminability, as we would not
225 necessarily expect that timepoints very early on in a trial (immediately after image onset) would produce
226 high discrimination between categories. We also reasoned that the best timepoint(s) may differ from par-
227 ticipant to participant depending on their electrode coverage. Therefore, we devised a participant-specific
228 timepoint feature selection process. Importantly, these feature selection steps were conducted within the
229 memory phase data (the same data on which the templates were trained), which were independent of the
230 test data of interest (encoding phase data).

231 We constructed a set of 30 binary classifiers to distinguish among two categories of a given condition
232 (**Figure 3B**): A1-A2, A1-A3, A1-B1, A1-B2, A1-B3, A2-A3, A2-B1, A2-B2, A2-B3, A3-B1, A3-B2, A3-B3, B1-B2, B1-
233 B3, B2-B3, X1-X2, X1-X3, X1-X4, X1-X5, X1-X6, X2-X3, X2-X4, X2-X5, X2-X6, X3-X4, X3-X5, X3-X6, X4-X5, X4-X6,
234 X5-X6. We employed a linear support vector machine approach using the SVC function in Python's scikit-
235 learn module, with a penalty parameter of 1.00. We split our data into two-thirds training and one-third
236 test (all within the memory phase), and iterated over the three train-test splits.

237 In the first step of feature selection, we independently trained classifiers on a single timepoint (each
238 of the 138 timepoints within a trial) and tested each classifier on all 138 timepoints at test (**Figure 3C**). We
239 averaged the classification over the 138 test timepoints to assess how well training at every timepoint gen-
240 eralized to all other timepoints within a trial. We conducted this analysis for all 30 classifiers and averaged
241 performance over classifiers, yielding a mean classification performance associated with each training time-
242 point. For each participant, we then computed the rank order of timepoints with respect to their classifi-
243 cation, such that the first ranked timepoint was the one that yielded the highest classification, and the last
244 ranked (138th) timepoint is the one that yielded the lowest classification.

245 To identify the set of training timepoints producing the best category classification for a given participant,
246 we repeated the pairwise classification procedure above iteratively training on an increasing number of
247 timepoints, adding from highest to lowest ranked (**Figure 3D**). Thus, these classifiers ranged from training
248 on the single top timepoint, to all 138 timepoints. We again conducted this analysis for all 30 classifiers and
249 averaged performance across them, yielding a mean classification performance associated with the 138
250 sets of top-N timepoints. We ranked this classification performance again to determine which number of
251 top timepoints produced the highest classification. This number was used to define the templates.

252 *Template correlations*

253 Using the set of training timepoints for each participant determined in the feature selection process, we then
254 computed a neural template for each category (**Figure 3E**). We extracted the pattern of activity (i.e., a vector
255 containing electrode contact, time, and frequency) for all instances of a given category during the memory
256 phase, including both old and new images. We then averaged over the timepoints in that participant's

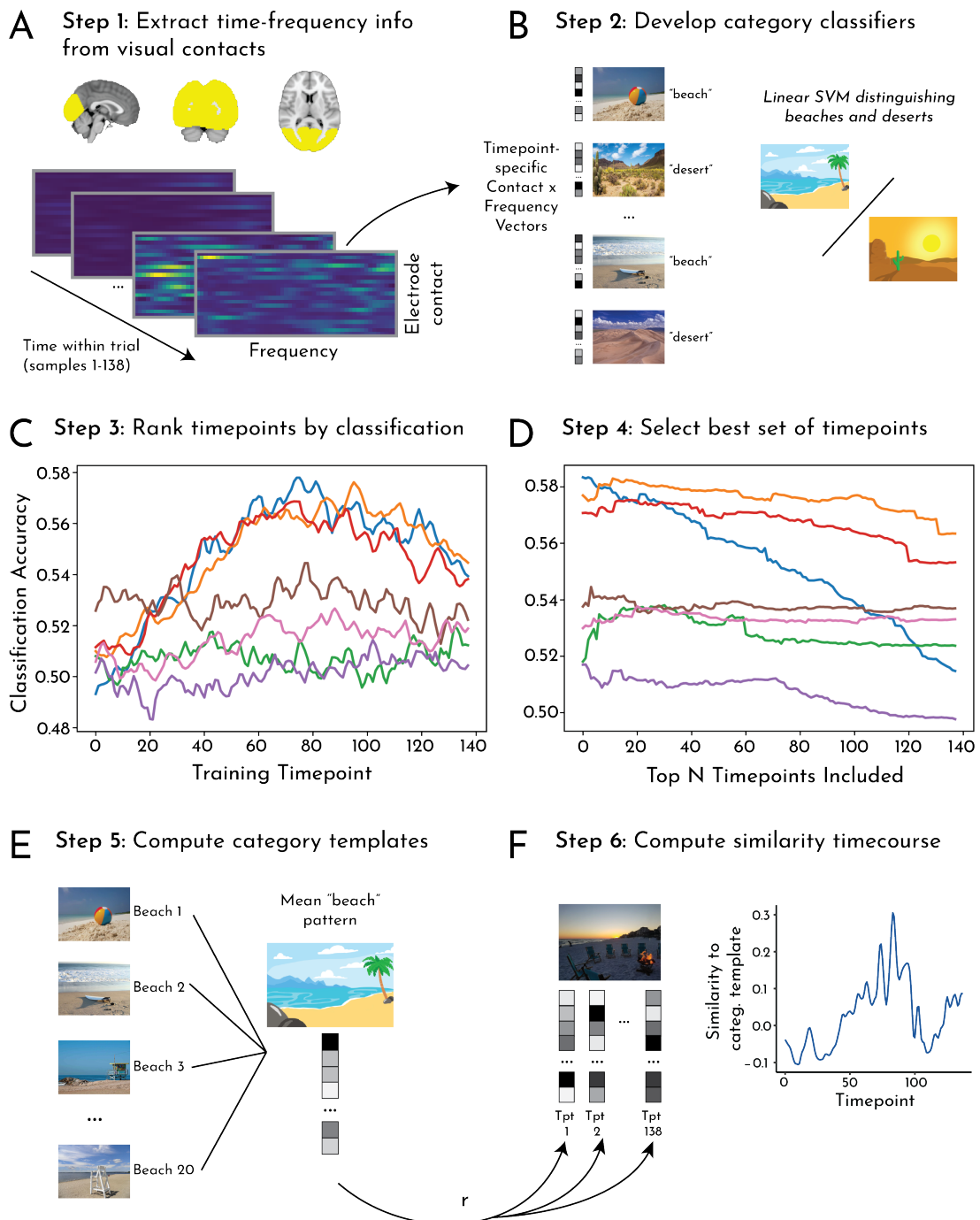


Figure 3. Category evidence analysis pipeline. (A) Step 1: A Morlet wavelet approach was used to extract time-frequency information from contacts in visual cortex. This resulted in contact by frequency vectors for every timepoint of encoding phase and memory phase trials, which served as the neural patterns for subsequent analysis steps. (B) Step 2: To identify the neural patterns that distinguished between categories, we ran a series of binary classifiers for every pair of categories from the memory phase trials. These classifiers were trained on the contact by frequency vectors for a single timepoint (Step 3) or set of timepoints (Step 4). The classifiers were then tested on timepoints from held-out data. (C) Step 3: As a first feature-selection step, we trained and tested the classifiers described in Step 2 separately for all individual timepoints. We then computed the average classification accuracy (across pairwise classifiers) for each timepoint and participant (each colored line indicates one participant). We then ranked the timepoints by classification accuracy. (D) Step 4: To select the set of timepoints that produced the best classification for a given participant, we trained and tested the classifiers in Step 2 on an increasing number of timepoints, starting with the best-performing timepoint identified in Step 3 and iteratively adding timepoints by rank. We then computed the per-participant average classification accuracy for each set of timepoints. (E) Step 5: We chose the per-participant top-N timepoint set that produced the best classification accuracy in Step 4, and then averaged contact by frequency vectors across those timepoints (across all exemplars of a given category) to create a "template" of neural activity for each category. (F) Step 6: We then correlated the template for each category from the memory phase with the contact by frequency vector at each timepoint of each trial/exemplar from that category during the (independent) encoding phase, yielding a timecourse of pattern similarity reflecting neural category evidence.

259 training set. The resulting category pattern vector retained spatial (contact) and frequency information.
260 To assess the timecourse of neural evidence for a category during the encoding phase, we extracted
261 the pattern of activity (contact and frequency) for each timepoint of every trial of that category (**Figure 3F**).
262 We computed the Pearson correlation between the template and the activity pattern separately for each
263 timepoint within a trial, yielding a timecourse of similarity to the template. The resulting Pearson correlation
264 values were Fisher transformed into z values.

265 We were interested in characterizing the timecourse of a category response not only while that category
266 was on the screen, but also during the surrounding trials. We may observe evidence for a category before
267 it appears, if it can be predicted (as hypothesized for B), or after it disappears, if its representation lingers.
268 Thus, we assessed the timecourse over a window comprising the on-screen category's trial ("Current") and
269 the two neighboring trials ("Pre" and "Post" trials). To quantify the response, we subtracted a baseline of
270 average evidence for the other categories of the same condition (e.g., for category A1, how much evidence
271 is there for A1 relative to categories A2 and A3?). For the X categories, which could appear in any order, we
272 ensured that the categories included in the baseline did not appear during the "Pre" and "Post" trials.

273 We quantified how template similarity changed over time within trial by splitting the trials into "ON" and
274 "ISI" epochs. The ON epoch refers to the part of the trial when the image was on the screen (the first 69
275 samples, or 267 ms). The ISI epoch refers to the part of the trial after the image disappeared from the screen
276 during the inter-stimulus fixation cross (the second 69 samples, or latter 267 ms).

277 *Subsequent memory*

278 To assess how variance in category evidence across trials related to memory outcomes for those trials,
279 we examined predictive and on-screen representations separately for subsequently remembered versus
280 forgotten trials. We conducted this analysis separately for memory of A (as a function of Perceived evidence
281 for A during A and Predicted evidence for B during A) and for memory of B (as a function of Perceived evidence
282 for B during B and Predicted evidence for B during A). Because each image was shown four times,
283 we first averaged the Perceived and Predicted evidence over these four trials. We considered the ISI epoch
284 of each trial, as this was the epoch in which we observed reliable evidence for the Predicted category B
285 during A. As a control analysis, we repeated these steps for the X trials from the Random blocks.

286 **Statistical analysis**

287 For all analyses (both behavioral and neural), statistical significance was assessed using a random-effects
288 bootstrap resampling approach (*Efron and Tibshirani, 1986*). For each of 10,000 iterations, we randomly
289 resampled participants with replacement and recomputed the mean across participants, to populate a sam-
290 pling distribution of the effect. This sampling distribution was used to obtain 95% confidence intervals and
291 perform null hypothesis testing. We calculated the *p*-value as the proportion of iterations in which the re-
292 sampled mean was in the wrong direction (opposite sign) of the true mean; we then multiplied these values
293 by 2 to obtain a two-tailed *p*-value. All resampling was done in R (version 3.4.1), and the random number
294 seed was set to 12345 before each resampling test. This approach is designed to assess the reliability of
295 effects across patients: a significant effect indicates that which patients were resampled on any given itera-
296 tion did not affect the result, and thus that the patients were interchangeable and the effect reliable across
297 the sample.

298 **Results**

299 **Memory behavior**

300 We first assessed overall performance in the recognition memory test to verify that participants were able
301 to encode the images into memory. We computed A', a non-parametric measure of sensitivity, from test
302 judgments for items from both Structured and Random blocks. All participants had an A' above the chance
303 level of 0.5 (mean = 0.68; 95% CI = [0.64, 0.70], *p* < 0.001; **Figure 4A**) indicating reliable memory. This was
304 driven by a higher hit rate (mean = 0.51) than false alarm rate (mean = 0.32; difference 95% CI = [0.14, 0.23], *p*
305 < 0.001). The proportions of items that were subsequently remembered (hit rate) or forgotten (1-hit rate, or

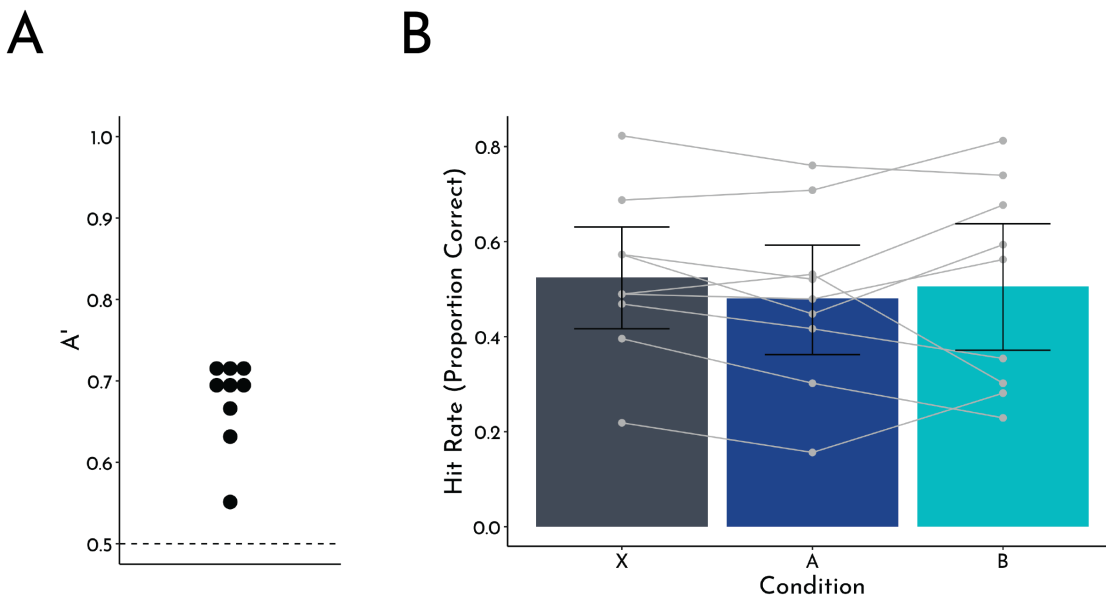


Figure 4. Behavioral results. (A) Overall memory performance collapsed across conditions. A' (a sensitivity measure for recognition memory) is depicted for each participant as a circle. All participants were above chance (0.5). (B) Hit rate as a function of condition (A: predictive; B: predictable; X: control). Group means are plotted as bars, with error bars representing the bootstrapped 95% confidence interval across participants. Individual participant data are overlaid with the grey circles and lines.

misses) were roughly matched on average, yielding balanced power for within-subject subsequent memory analyses.

We then assessed how statistical learning affected recognition memory. Based on our prior work (*Sherman and Turk-Browne, 2020*), we hypothesized that the hit rate for items from the predictive A categories in the Structured blocks would be lower than the hit rate for items from the control X categories in the Random blocks. Indeed, we replicated this key behavioral finding (**Figure 4B**), with a significantly lower hit rate for A (mean = 0.48) than X (mean = 0.52; difference 95% CI = [-0.076, -0.010], $p = 0.012$). The hit rate for B (mean = 0.51) did not differ from A (difference 95% CI = [-0.10, 0.059], $p = 0.51$) or X (difference 95% CI = [-0.094, 0.053], $p = 0.66$).

The false alarm rate for X (mean = 0.36) was numerically higher than A (mean = 0.28; difference 95% CI = [-0.0023, 0.16], $p = 0.064$); X was significantly higher than B (mean = 0.29; difference 95% CI = [0.0069, 0.13], $p = 0.028$), though A and B did not differ (difference 95% CI = [-0.074, 0.056], $p = 0.82$). Unlike the higher hit rate for X than A, which was specifically hypothesized based on prior work, the marginally higher false alarm rate for X than A was not expected or consistent with previous experiments. Nevertheless, this complicates interpretation of the hit rate difference as impaired memory for A vs. X. One difference from the prior study is the blocking of Structured (A,B) and Random (X) categories, which may have allowed for differences in strategy or motivation between conditions. Nevertheless, the main memory hypotheses in the current study rest within the A condition (i.e., which A items are remembered vs. forgotten as a function of B prediction), rather than on overall condition-wide differences with X (or B).

325 Neural frequency tagging

To provide a neural check of statistical learning of the category pairs in the Structured blocks, we measured entrainment of neural oscillations in visual electrode contacts to the frequency of individual images and image pairs (**Figure 5A**). We expected strong entrainment at the image frequency in both the Structured and Random blocks, as this reflects the periodicity of the sensory stimulation. Critically, we hypothesized that there would be greater entrainment at the pair frequency in Structured compared to Random blocks. This provides a measure of statistical learning because the pairs only exist when participants extract regularities

A

Sensory Input



Image Frequency



Pair Frequency



B

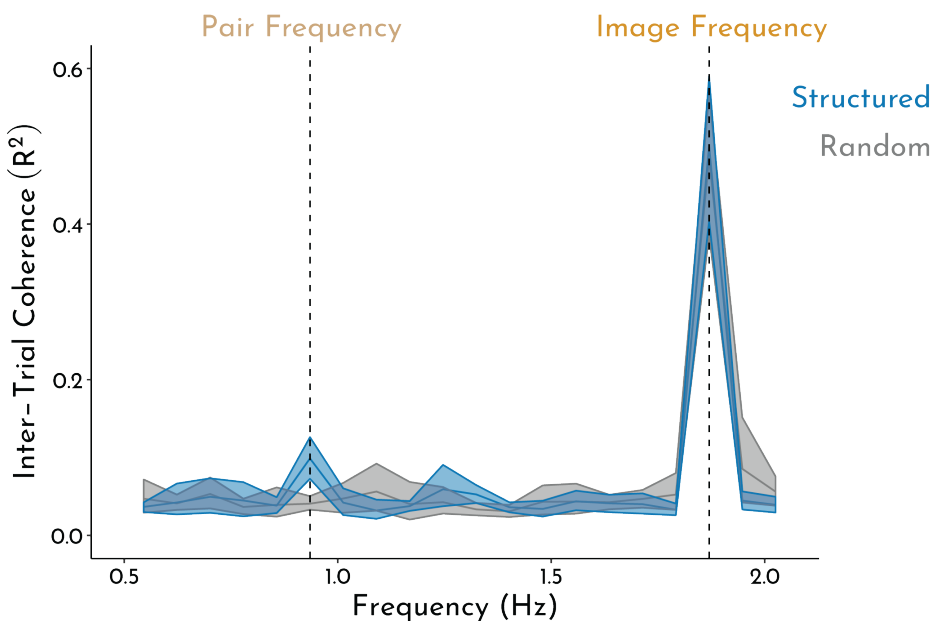


Figure 5. Neural frequency tagging analysis. (A) Schematic of analysis and hypothesized neural oscillations. We expect entrainment of visual contacts at the frequency of images in both blocks. In the Structured block, we also expect entrainment at the frequency of category pairs. (B) These hypotheses were confirmed, with reliable peaks in coherence at the image and pair frequencies in Structured blocks but only at the image frequency in Random blocks. Error bands indicate the 95% bootstrapped confidence intervals across participants.

332 over time in the transition probabilities between categories in the Structured blocks.

333 Consistent with our hypotheses and prior work (*Henin et al., 2021*), there were distinct peaks in phase
334 coherence at both the image and pair frequencies in Structured blocks, but only at the image frequency in
335 Random blocks (**Figure 5B**). To confirm the reliability of these peaks, we contrasted the coherence at the
336 frequency of interest (image: 1.87 Hz; pair: 0.93 Hz) against a baseline of the coherence at frequencies
337 neighboring each of the frequencies of interest (± 0.078 Hz). At the image frequency, there were reliable
338 peaks in both the Structured (mean difference = 0.46; 95% CI = [0.37, 0.55], $p < 0.001$) and Random blocks
339 (mean difference = 0.42; 95% CI = [0.28, 0.52], $p < 0.001$). At the pair frequency, there was a reliable peak
340 in Structured blocks (mean difference = 0.059; 95% CI = [0.035, 0.084], $p < 0.001$), but not Random blocks
341 (mean difference = -0.0027; 95% CI = [-0.016, 0.0085], $p = 0.68$).

342 Further, the peak in coherence at the pair frequency in Structured blocks was reliably higher than that in
343 Random blocks (mean difference = 0.058; 95% CI = [0.035, 0.083], $p < 0.001$), confirming the pair frequency
344 effect was specific to when there was structure in the sequence. There were no differences in coherence at
345 the image frequency across conditions (mean difference = 0.018; 95% CI = [-0.010, 0.048], $p = 0.25$). Together,
346 these results provide strong evidence that visual regions represented the paired categories during statistical
347 learning.

348 **Neural category evidence**

349 The neural frequency tagging for pairs in Structured blocks indicates statistical learning of the pairs. This
350 learning should create predictive value for the items from the A categories, which afford a prediction of
351 the associated B category. To test for these predictive representations, we employed a multivariate pattern
352 similarity approach that extracted neural evidence for visual categories. For each category, we created a
353 neural template based on the pattern of time-frequency information evoked by each category across visual
354 contacts. We then quantified the expression of these templates in the Structured and Random blocks. As a
355 check, we expected clear neural evidence for the category of the item being presented on the screen.

356 Critically, we hypothesized that neural evidence for the upcoming B category would manifest before
357 its appearance, in response to an A exemplar. We measured these temporal dynamics of neural category
358 evidence by creating a window of three trials centered on the current item: the trial preceding a trial in
359 which the item appeared ("Pre"), the trial during which the item was on the screen ("Current"), and the trial
360 succeeding the trial in which the item appeared ("Post"). For example, if category Pair 1 involved beaches (A1)
361 being followed by mountains (B1), neural evidence for the mountain category was calculated in response to
362 beach exemplars (Pre), mountain exemplars (Current), and exemplars from the categories that could appear
363 next in the Structured sequence (A2 or A3 categories). These evidence values were averaged across the
364 categories from the same condition (e.g., B1, B2, and B3 for condition B) and plotted over time (**Figure 6A**).
365 For statistical analysis, we averaged the neural category evidence for each category across the timepoints
366 within 6 epochs: when Pre, Current, and Post images were on the screen ("ON") and during the fixation
367 period between these trials ("ISI"; **Figure 6B**). We anticipated the evoked response to each image would span
368 ON and ISI periods (as neural processing of the image would take longer than 267 ms), but subdividing in
369 this way allowed us to test for the emergence of predictive evidence of B during the ISI immediately prior
370 to its onset.

371 For Current trials (i.e., the trial when the target category was on screen), we found robust (perceptual)
372 evidence for both A and B across both the ON epoch (A: mean = 0.0088; 95% CI = [0.0046, 0.013], $p < 0.001$;
373 B: mean = 0.012; 95% CI = [0.0066, 0.018], $p < 0.001$) and ISI epoch (A: mean = 0.012; 95% CI = [0.0084,
374 0.015], $p < 0.001$; B: mean = 0.014; 95% CI = [0.0083, 0.019], $p < 0.001$). Neural evidence for X categories
375 from Random blocks was not reliable during the ON epoch (mean = 0.0046, 95% CI = [-0.00075, 0.012], p
376 = 0.13) but became robust later in the trial during the ISI epoch (mean = 0.0074; 95% CI = [0.0030, 0.013],
377 $p < 0.001$). There was greater evidence for B than X categories during both ON (mean difference = 0.0077;
378 95% CI = [0.00058, 0.015], $p = 0.031$) and ISI epochs (mean difference = 0.0065; 95% CI = [0.00061, 0.012], p
379 = 0.031). Considering X as a baseline, this difference shows enhanced perceptual processing of predictable
380 categories. Neural evidence did not differ between A and B categories ($ps > 0.38$) or A and X categories (ps
381 > 0.28).

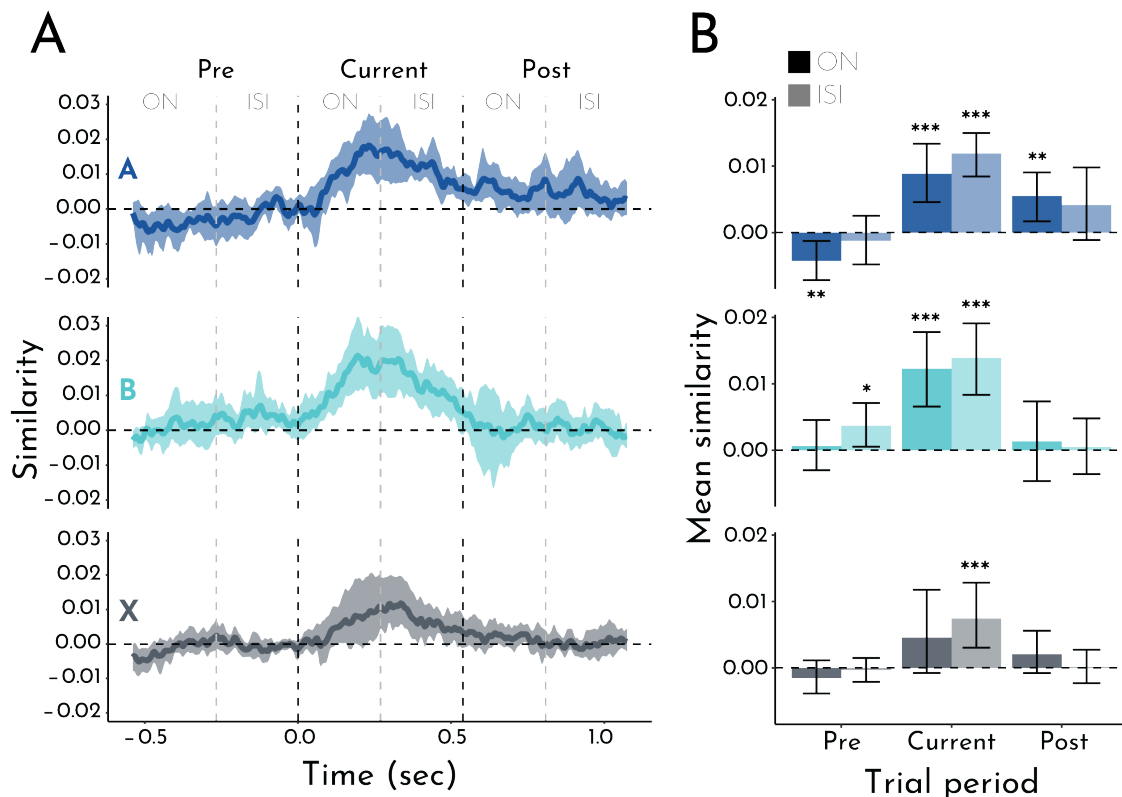


Figure 6. Neural category evidence. (A) Time course of similarity between patterns of neural activity in visual contacts evoked by exemplars from A (predictive), B (predictable), and X (control) categories and category template patterns for A, B, and X. Current refers to the trial when the item was presented, Pre refers to the trial before the item was presented, and Post refers to the trial after the item was presented. For each row/condition, the Pre, Current, and Post trials are compared to the same category template (Current). Error bands reflect the bootstrapped 95% confidence intervals across participants (i.e., any timepoint whose band excludes 0, $p < 0.05$). (B) Average pattern similarity collapsed across timepoints within ON (stimulus on screen) and ISI (fixation between stimuli) epochs. Bars represent the means across participants and error bars indicate the bootstrapped 95% confidence intervals. * $p < 0.05$; ** $p < 0.01$; *** $p < 0.001$

382 For Pre trials (i.e., the trial before the target category appeared), we found the hypothesized predictive
383 neural evidence for the B categories during the ISI epoch (just after its paired A category appeared; mean =
384 0.0037; 95% CI = [0.00054, 0.0071], $p = 0.019$). B evidence was not present during the ON epoch earlier in the
385 Pre trials (while its paired A category was on screen; mean = 0.00063; 95% CI = [-0.0030, 0.0046], $p = 0.78$);
386 this may reflect the time needed for associative reactivation of the B category after perceptual processing of
387 the A item, or anticipation of the timing when B will appear (at the end of the Pre trial). Further supporting
388 our interpretation that Pre evidence of the B categories reflects prediction, no such evidence was observed
389 for X during ON (mean = -0.0015; 95% CI = [-0.0039, 0.0012], $p = 0.26$) or ISI epochs (mean = -0.00031; 95%
390 CI = [-0.0021, 0.0015], $p = 0.73$) or for A during the ISI epoch (mean = -0.0012; 95% CI = [-0.0048, 0.0025], $p =$
391 0.53). There was *negative* evidence for the upcoming A category during the ON epoch of the Pre trial (mean
392 = -0.0043; 95% CI = [-0.0072, -0.0013], $p = 0.0052$), but this may have been artifactual (see below). When
393 contrasting prediction-related signals across conditions, Pre neural evidence for the B categories during
394 the ISI epoch was reliably greater than X categories (mean difference = 0.0040; 95% CI = [0.00016, 0.0075],
395 $p = 0.042$) and marginally greater than A categories (mean difference = 0.0049; 95% CI = [-0.00051, 0.010],
396 $p = 0.075$).

397 For Post trials (i.e., the trial after the target category appeared), we found reliable neural evidence for
398 the A categories during the ON epoch (i.e., while its paired B category was on screen; mean = 0.0055; 95%
399 CI = [0.0017, 0.0091], $p = 0.0018$); this effect was not significant during the ISI epoch (mean = 0.0041; 95%
400 CI = [-0.0011, 0.0098], $p = 0.13$). We did not find Post evidence of B or X categories during either ON or ISI
401 epochs ($p > 0.80$), nor was Post evidence for A reliably stronger than B or X ($p > 0.16$). Positive evidence of A
402 during the Post trial may be related to the negative evidence of A during the Pre trial noted above. Because
403 no back-to-back pair repetitions were allowed, in an A1-B1-A2-B2 trial sequence, A1 and A2 were different
404 categories. A1 evidence during B1 was considered a Post trial for the A condition, whereas A2 evidence
405 during B1 was considered a Pre trial for the A condition. Because A1 was one of two baseline categories for
406 A2 (along with the third A category, A3), Post evidence for A1 during B1 would have been subtracted from
407 Pre evidence for A2, leading to a negative effect. We tested this by comparing evidence for A2 (Pre) and A1
408 (Post) during B1 to the neutral A3 only. This weakened the negative Pre evidence for A, during ON (mean =
409 -0.0027; 95% CI = [-0.0054, 0.00], $p = 0.058$) and ISI epochs (mean = 0.00048; 95% CI = [-0.0022, 0.0038], $p =$
410 0.82). However, the positive Post evidence for A during the ON epoch remained significant (mean = 0.0081;
411 95% CI = [0.0036, 0.014], $p < 0.001$).

412 Taken together, these results show that statistical learning of the category pairs in Structured blocks
413 affected neural representations in the task. Not only did visual contacts represent the category of the first
414 and second items in a pair while they were being perceived (A and B evidence during ON and ISI epochs of
415 A and B, respectively), but also the first category during the second (A evidence during ON epoch of B) and
416 the second category during the first (B evidence during ISI epoch after A). This latter effect indicates that
417 the first item in a pair (from A category) had predictive value on average.

418 Subsequent memory analysis

419 We theorized that items with predictive value are a lower priority for new encoding into episodic memory.
420 Here we test this relationship by comparing neural category evidence for remembered vs. forgotten items
421 within participants. That is, although A items had reliable predictive value on average, variability across
422 items may relate to subsequent memory. To the extent that prediction interferes with encoding, we hy-
423 pothesized that subsequently forgotten A items would elicit evidence for the upcoming B category during
424 their encoding.

425 Consistent with our hypothesis, B evidence during the ISI epoch after A (i.e., Predicted category) was
426 negatively related to subsequent A memory (**Figure 7A**): forgotten A items yielded reliable B evidence (mean
427 = 0.0092; 95% CI = [0.0023, 0.017], $p = 0.0030$), whereas remembered A items did not (mean = 0.0017; 95%
428 CI = [-0.0016, 0.0049], $p = 0.31$). In contrast, A evidence during the ISI epoch after A (i.e., Perceived category)
429 was reliable for both remembered (mean = 0.012; 95% CI = [0.0091, 0.015], $p < 0.001$) and forgotten (mean =
430 0.014; 95% CI = [0.0077, 0.021], $p < 0.001$) A items. This differential effect of subsequent memory on neural
431 evidence for Perceived vs. Predicted categories during the ISI after A was reflected in a significant 2 (evidence

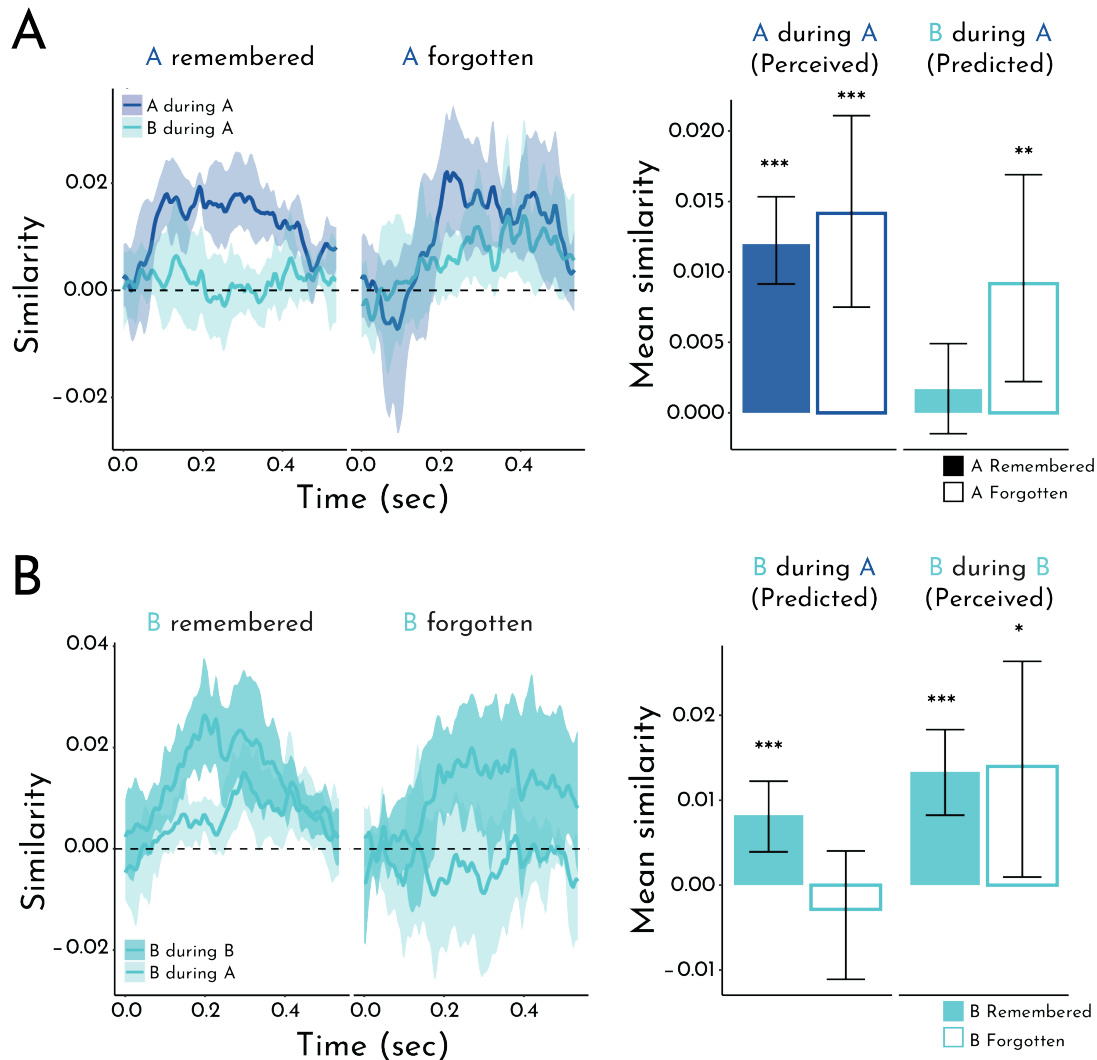


Figure 7. Subsequent memory analysis. A) Left: Timecourse of pattern similarity in visual contacts between A items being encoded and the Perceived A (A during A) and Predicted B (B during A) category templates, as a function of whether A items were subsequently remembered or forgotten. Right: Pattern similarity averaged within the ISI period, the epoch in which we observed overall evidence of prediction, as a function of subsequent memory for A items (filled bars = remembered; empty bars = forgotten). B) Left: Timecourse of pattern similarity in visual contacts between B items being encoded and the Predicted B (B during A) and Perceived B (B during B) category templates, as a function of whether B items were subsequently remembered for forgotten. Right: Pattern similarity averaged within the ISI period, as a function of subsequent memory for B items. Error shading/bars reflect the bootstrapped 95% confidence interval across participants. * $p < 0.05$; ** $p < 0.01$; *** $p < 0.001$

432 category: A, B) by 2 (subsequent memory: remembered, forgotten) interaction ($p < 0.001$). This interaction
433 was driven by a marginal difference in neural evidence for the Predicted B category during encoding of
434 subsequently forgotten vs. remembered A items (mean difference = 0.0075; 95% CI = [-0.00046, 0.016], p
435 = 0.065), but no reliable difference in neural evidence for the Perceived A category by subsequent memory
436 (mean difference = 0.0022; 95% CI = [-0.0050, 0.0094], p = 0.57).

437 As a control analysis, we performed the key steps above in the Random blocks. These blocks did not
438 contain pairs, and so we dummy-coded pairs of X items (X_1 - X_2 instead of A-B). In contrast to Structured
439 blocks, we did not expect that neural evidence of the “Predicted” X_2 category during the X_1 ISI would relate
440 to subsequent memory for X_1 . Indeed, there was no reliable evidence for the X_2 category for either remem-
441 bered (mean = -0.0029; 95% CI = [-0.0069, 0.00084], p = 0.14) or forgotten (mean = 0.0011; 95% CI = [-0.0027,
442 0.0054], p = 0.57) X_1 items. In contrast, neural evidence for the Perceived X_1 category during the X_1 ISI was
443 reliable for both remembered X_1 items (mean = 0.010; 95% CI = [0.0039, 0.019], $p < 0.001$) and forgotten X_1
444 items (mean = 0.0065; 95% CI = [0.0022, 0.012], $p < 0.001$).

445 We so far focused on the effects of prediction for memory of the item generating the prediction (A), but
446 what is the mnemonic fate of the item being predicted (B), which in this task with deterministic pairs always
447 appeared as expected? Whereas neural category evidence for B during the A ISI (Predicted) was negatively
448 related to subsequent memory for A items, the opposite was true for memory of B items (**Figure 7B**): re-
449 membered B items were associated with reliable prediction of B (mean = 0.0082; 95% CI = [0.0036, 0.012], p
450 <0.001), but forgotten B items were not (mean = -0.0028; 95% CI = [-0.011, 0.0041], p = 0.49). In contrast, and
451 similar to A memory, evidence for B during the B ISI (Perceived) was reliable for both remembered (mean =
452 0.013; 95% CI = [0.0082, 0.018], $p < 0.001$) and forgotten (mean = 0.014; 95% CI = [0.00096, 0.026], p = 0.034)
453 B items. We did not find an interaction between category and memory (p = 0.22). However, there was a
454 reliable difference in Predicted B evidence for remembered vs. forgotten B items (mean difference = 0.011;
455 95% CI = [0.00060, 0.021], p = 0.039); Perceived B evidence did not differ as a function of memory (mean
456 difference = 0.00064; 95% CI = [-0.014, 0.016], p = 0.89).

457 We repeated the same control analysis of Random blocks, but now focused on subsequent memory for
458 X_2 items (equivalent to B, rather than X_1 memory for A). Neural evidence for the “Predicted” X_2 category
459 during the ISI after X_1 was not reliable for either remembered (mean = 0.0013; 95% CI = [-0.0020, 0.0043], p
460 = 0.44) or forgotten (mean = -0.00048; 95% CI = [-0.0030, 0.0017], p = 0.75) X_2 items.

461 Together, these results highlight the opposing influence of predictive value on memory for predictive
462 versus predicted items. Namely, prediction of B (during A) is associated with worse memory for predictive
463 A items (suggesting interference between the generation of a prediction and encoding of the current item)
464 but better memory for predicted B items (suggesting that this prediction may potentiate encoding of an
465 upcoming item).

466 Discussion

467 This study demonstrates a trade-off between how well an item is encoded into episodic memory and how
468 strong of a future prediction it generates based on statistical learning. We first used frequency tagging
469 to provide neural verification of statistical learning. During a sequence of scene photographs, electrodes
470 in visual cortex represented pairs of scene categories that reliably followed each other, synchronizing not
471 only to the individual scenes but also to the boundaries between pairs. Next, we used multivariate pattern
472 analysis to assess how the paired categories were represented over time. Items from the first category in a
473 pair elicited a representation of the second category, which grew in strength in advance of the onset of items
474 from the second category. We refer to the ability of an item to generate this predictive representation as its
475 “predictive value”. Critically, by relating these representational dynamics to subsequent memory behavior,
476 we found that forgotten items from the first category triggered reliable predictions during encoding whereas
477 remembered first items had not.

478 Our work builds upon suggestive evidence from a prior study that predictive value may influence sub-
479 sequent memory (*Sherman and Turk-Browne, 2020*). This prior study included behavioral and fMRI experi-
480 ments, whereas the current study employed iEEG. Neural measures are an important advance over behav-
481 ior alone because they can assay predictive representations during passive viewing at encoding. iEEG is

482 superior to fMRI for this purpose because neural activity is sampled at much greater temporal resolution
483 and activity reflects instantaneous electrical potentials rather than hemodynamic responses smoothed and
484 delayed in time. This provides much greater confidence that the upcoming category was being represented
485 *prior* to its appearance and thus was truly predictive. Moreover, the prior study showed a negative rela-
486 tionship between prediction and memory across participants, whereas the current study established this
487 relationship within participant. This is also an important advance because an across-participant relation-
488 ship does not provide strong evidence for the claim that prediction during encoding impairs memory. Such
489 a relationship could reflect generic individual differences such that, for example, a participant with better
490 overall memory generates the same weak prediction on both remembered and forgotten trials. In contrast,
491 in this study we were able to link prediction to successful vs. unsuccessful memory formation across items.
492 This more sensitive approach yielded other findings not observed in the prior study, including that memory
493 for B items had an opposite, positive relationship with prediction of B. Taken together, these results pro-
494 vide mechanistic insight into the interaction between predictive value and memory, and speak to theoretical
495 questions about the representations underlying statistical learning and episodic memory.

496 **Nature of representational changes**

497 Several fMRI studies have shown that statistical and related forms of learning can change neural represen-
498 tations of associated items throughout the human brain (*Schapiro et al., 2012, 2013; Schlichting et al., 2015;*
499 *Deuker et al., 2016; Tompary and Davachi, 2017*). For example, if exposed to sequential pairs embedded
500 in a continuous stream of objects (akin to the category pairs in the current study), the two objects in a pair
501 come to elicit more similar patterns of fMRI activity from before to after learning, when presented on their
502 own, in the medial temporal lobe cortex and hippocampus (*Schapiro et al., 2012*). Such integration could
503 be interpreted as evidence that the representations of the paired items merged into a single “unitized” rep-
504 resentation of the pair that can be evoked by either item (*Fujimichi et al., 2010*). Alternatively, the paired
505 items may remain distinct but become associated, such that either can be reactivated by the other through
506 spreading activation (*Schapiro et al., 2017*). A key difference between these accounts is the timing of how
507 learned representations emerge when one of the items is presented: the merging account predicts that
508 the (same) unitized representation is evoked immediately by either paired item, whereas the associative
509 account predicts that the presented item is represented immediately while the paired item is represented
510 gradually over time through reactivation. These dynamics cannot be distinguished by fMRI because of its
511 slow temporal resolution, but our iEEG approach may shed light.

512 On the surface, the results of our frequency tagging analysis may seem to suggest a merged represen-
513 tation of the category pairs. The reliable peak in coherence at the frequency of two consecutive stimuli may
514 suggest that electrodes in visual cortex represented the paired categories as a single unit (*Batterink and*
515 *Paller, 2017*). However, the results of our pattern similarity analysis are more consistent with an association
516 between the paired categories. Although we found that both categories in a pair could be represented at
517 the same time (i.e., predictive B evidence during the A Pre trial and lingering A evidence during the B Post
518 trial, relative to no such evidence on X trials), these representations were offset in time. The representation
519 of the A category was robust during both the ON and ISI epochs of the A trial, whereas the representa-
520 tion of the B category was not reliable during the ON epoch and only emerged during the ISI epoch. Thus,
521 our results are more consistent with an associative account in visual cortex. It remains possible that the
522 hippocampus or other brain structures represent statistical regularities through unitized representations.
523 Moreover, one limitation of our study is that we did not measure representations of individual categories
524 before and after learning to directly assess representational change. Though note that this is more impor-
525 tant for fMRI where, unlike with iEEG, the coarse temporal resolution makes it difficult to separate neural
526 responses of paired stimuli during statistical learning.

527 **Predictive interference on memory encoding**

528 The timecourse of predictive representations also sheds light on the temporal dynamics of the interaction
529 between episodic memory and statistical learning. When examining the overall effect of prediction, we
530 found reliable B evidence during the ISI epoch of A, immediately preceding the appearance of B. However,

531 this result was obtained by averaging across all trials, both remembered and forgotten. Thus, it was possible
532 that when separated out by subsequent memory, a different pattern would emerge. One possibility is that B
533 evidence would come online earlier for forgotten items, which might suggest that the observed impairment
534 in A memory resulted from interference with perceptual processing of A. To the contrary, the difference
535 in B evidence for remembered vs. forgotten A items was clearest during the ISI after A was removed from
536 the screen, which suggests that prediction may interfere with later, post-perceptual stages of processing to
537 impair encoding.

538 Interestingly, evidence for the current A category was comparable across remembered and forgotten
539 A items. Thus, in this paradigm, variance in memory was explained solely by prediction of the upcoming
540 category, not the strength of perceptual processing of the category being encoded (*Kuhl et al., 2012*) nor
541 modulation of this processing by prediction (both of which would have affected A evidence). The lack of a
542 relationship between A evidence and A memory may reflect a tradeoff: category evidence may reflect rep-
543 resentation of the most diagnostic features of a category, which would enhance memory for these features
544 while impairing memory for idiosyncratic features of particular exemplars. A related account may explain
545 why predictive B evidence was positively linked to B memory (*Smith et al., 2013; Thavabalasingam et al.,*
546 *2016*): B evidence during the A ISI may potentiate the diagnostic features of the B category, enhancing the
547 salience of idiosyncratic features of B when it appears to strengthen episodic memory for B. Future studies
548 could test these possibilities by using a more continuous measure of memory precision and by testing on
549 modified items that retain category-diagnostic vs. idiosyncratic features.

550 This work builds on existing theories considering the complex interplay between memory encoding and
551 memory retrieval. To the extent that prediction from statistical learning can be considered as "retrieval"
552 of an associated memory (*Kok and Turk-Browne, 2018; Hindy et al., 2016*), our findings converge with the
553 notion that the brain cycles between mutually exclusive encoding and retrieval states (*Hasselmo et al., 2002*;
554 *Duncan et al., 2012; Long and Kuhl, 2019; Bein et al., 2020*). Further, a recent computational model suggests
555 that predictive uncertainty determines when memories should be encoded or retrieved (*Lu et al., 2022*). The
556 model accounts for findings that familiar experiences are more likely to evoke retrieval (*Patil and Duncan,*
557 *2018*), and thus may help to explain why predictions from statistical learning are prioritized over episodic
558 encoding.

559 Neural source of predictions

560 The current study sought to decode evidence of visual categories and so focused on electrode contacts in
561 visual cortex. This adds to a growing literature on predictive signals in visual cortex (*De Lange et al., 2018;*
562 *Kim et al., 2020*). However, these signals may originate elsewhere in the brain. A strong candidate is the
563 hippocampus and surrounding medial temporal lobe cortex. In addition to representing predictions (*Kok*
564 *and Turk-Browne, 2018; Sherman and Turk-Browne, 2020*), the hippocampus interfaces between perception
565 and memory (*Treder et al., 2021*) and has been shown to drive reinstatement of predicted information in
566 visual cortex (*Bosch et al., 2014; Tanaka et al., 2014; Danker et al., 2017; Hindy et al., 2016*).

567 Beyond generating predictions, the hippocampus may also be the nexus of the interaction between
568 episodic memory and statistical learning, given its fundamental role in both functions (*Schapiro et al., 2017*).
569 Indeed, given the necessity of the hippocampus for episodic memory, our study raises questions about how
570 the representations of perceived and predicted categories in visual cortex are routed into the hippocam-
571 pus for encoding. One intriguing possibility is that these representations are prioritized according to biased
572 competition (*Desimone, 1998; Hutchinson et al., 2016*), leading to preferential routing and subsequent en-
573 coding of predicted, but not perceived, information in the hippocampus. Relatedly, recent work had found
574 that encoding vs. retrieval states are associated with distinct patterns of activity in visual cortex (*Long and*
575 *Kuhl, 2021*), suggesting that representations in visual regions may be fundamentally shaped by memory
576 state in the hippocampus.

577 The patients in the current study had relatively few contacts in the hippocampus and medial temporal
578 lobe cortex, precluding careful analysis of prediction in these regions and how it relates to visual cortex.
579 Future studies with a larger cohort of patients and/or high-density hippocampal recordings would be useful
580 for this purpose. Likewise, future studies could disrupt the hippocampus through stimulation to establish

581 its causal role in predictive representations in visual cortex.

582 Conclusion

583 In examining the trade-off between prediction and memory encoding, our work suggests a novel theoretical
584 perspective on why predictive value shapes memory. We argue that because memory is capacity- and
585 resource-limited, memory systems must prioritize which information to encode. When prior statistical learning
586 enables useful prediction of an upcoming experience, that prediction takes precedence over encoding.
587 In this way, encoding is focused adaptively on experiences for which there is room to develop stronger
588 predictions.

589 Acknowledgments

590 We are grateful to the patients who participated in this study. We thank Kun Wu for providing the elec-
591 trode reconstructions, Christopher Benjamin for helping to recruit patients and coordinate testing, Richard
592 Aslin and Sami Yousif for helpful conversations, and Gregory McCarthy for advice about data collection and
593 analysis, as well as for feedback on the manuscript. This work was supported by NIH grant R01 MH069456
594 (N.B.T-B.), the Canadian Institute for Advanced Research (N.B.T-B.), and an NSF GRFP grant (B.E.S).

595 Competing Interests

596 The authors declare no competing interests.

597 References

598 **Aitken F**, Turner G, Kok P. Prior expectations of motion direction modulate early sensory processing. *Journal of Neuro-
599 science*. 2020; 40(33):6389–6397.

600 **Aly M**, Turk-Browne NB. How hippocampal memory shapes, and is shaped by, attention. In: *The hippocampus from cells
601 to systems* Springer; 2017.p. 369–403.

602 **Batterink LJ**, Paller KA. Online neural monitoring of statistical learning. *Cortex*. 2017; 90:31–45.

603 **Bein O**, Duncan K, Davachi L. Mnemonic prediction errors bias hippocampal states. *Nature communications*. 2020;
604 11(1):1–11.

605 **Bein O**, Plotkin NA, Davachi L. Mnemonic prediction errors promote detailed memories. *Learning and Memory*. 2021; .

606 **Biderman N**, Bakkour A, Shohamy D. What are memories for? The hippocampus bridges past experience with future
607 decisions. *Trends in Cognitive Sciences*. 2020; 24(7):542–556.

608 **Bosch SE**, Jehee JF, Fernández G, Doeller CF. Reinforcement of associative memories in early visual cortex is signaled by
609 the hippocampus. *Journal of Neuroscience*. 2014; 34(22):7493–7500.

610 **Brady TF**, Oliva A. Statistical learning using real-world scenes: Extracting categorical regularities without conscious intent.
611 *Psychological science*. 2008; 19(7):678–685.

612 **Choi D**, Batterink LJ, Black AK, Paller KA, Werker JF. Preverbal Infants Discover Statistical Word Patterns at Similar Rates
613 as Adults: Evidence From Neural Entrainment. *Psychological Science*. 2020; 31(9):1161–1173.

614 **Cowan ET**, Schapiro AC, Dunsmoor JE, Murty VP. Memory consolidation as an adaptive process. *Psychonomic Bulletin &
615 Review*. 2021; 28(6):1796–1810.

616 **Danker JF**, Tompary A, Davachi L. Trial-by-trial hippocampal encoding activation predicts the fidelity of cortical reinstatement
617 during subsequent retrieval. *Cerebral Cortex*. 2017; 27(7):3515–3524.

618 **De Brigard F**. Is memory for remembering? Recollection as a form of episodic hypothetical thinking. *Synthese*. 2014;
619 191(2):155–185.

620 **De Lange FP**, Heilbron M, Kok P. How do expectations shape perception? *Trends in cognitive sciences*. 2018; 22(9):764–
621 779.

622 **Demarchi G**, Sanchez G, Weisz N. Automatic and feature-specific prediction-related neural activity in the human auditory
623 system. *Nature communications*. 2019; 10(1):1–11.

624 Desimone R. Visual attention mediated by biased competition in extrastriate visual cortex. *Philosophical Transactions of the Royal Society of London Series B: Biological Sciences*. 1998; 353(1373):1245–1255.

625

626 Deuker L, Bellmund JL, Schröder TN, Doeller CF. An event map of memory space in the hippocampus. *Elife*. 2016; 5:e16534.

627

628 Dickerson KC, Adcock RA. Motivation and memory. *Stevens' Handbook of Experimental Psychology and Cognitive Neuroscience, Learning and Memory*. 2018; 1:215.

629

630 Dolcos F, Katsumi Y, Weymar M, Moore M, Tsukiura T, Dolcos S. Emerging directions in emotional episodic memory. *Frontiers in Psychology*. 2017; 8:1867.

631

632 Duncan K, Sadanand A, Davachi L. Memory's penumbra: episodic memory decisions induce lingering mnemonic biases. *Science*. 2012; 337(6093):485–487.

633

634 Efron B, Tibshirani R. Bootstrap methods for standard errors, confidence intervals, and other measures of statistical accuracy. *Statistical science*. 1986; p. 54–75.

635

636 Endress AD, Johnson SP. When forgetting fosters learning: A neural network model for statistical learning. *Cognition*. 2021; p. 104621.

637

638 Fujimichi R, Naya Y, Koyano KW, Takeda M, Takeuchi D, Miyashita Y. Unitized representation of paired objects in area 35 of the macaque perirhinal cortex. *European Journal of Neuroscience*. 2010; 32(4):659–667.

639

640 Gebhart AL, Aslin RN, Newport EL. Changing structures in midstream: Learning along the statistical garden path. *Cognitive science*. 2009; 33(6):1087–1116.

641

642 Goldfarb EV. Enhancing memory with stress: progress, challenges, and opportunities. *Brain and Cognition*. 2019; 133:94–105.

643

644 Greve A, Cooper E, Kaula A, Anderson MC, Henson R. Does prediction error drive one-shot declarative learning? *Journal of memory and language*. 2017; 94:149–165.

645

646 Hasselmo ME, Bodelón C, Wyble BP. A proposed function for hippocampal theta rhythm: separate phases of encoding and retrieval enhance reversal of prior learning. *Neural computation*. 2002; 14(4):793–817.

647

648 Henin S, Turk-Browne NB, Friedman D, Liu A, Dugan P, Flinker A, Doyle W, Devinsky O, Melloni L. Learning hierarchical sequence representations across human cortex and hippocampus. *Science advances*. 2021; 7(8):eabc4530.

649

650 Hindy NC, Ng FY, Turk-Browne NB. Linking pattern completion in the hippocampus to predictive coding in visual cortex. *Nature neuroscience*. 2016; 19(5):665–667.

651

652 Hutchinson JB, Pak SS, Turk-Browne NB. Biased competition during long-term memory formation. *Journal of cognitive neuroscience*. 2016; 28(1):187–197.

653

654 Jenkinson M, Bannister P, Brady M, Smith S. Improved optimization for the robust and accurate linear registration and motion correction of brain images. *Neuroimage*. 2002; 17(2):825–841.

655

656 Jenkinson M, Beckmann CF, Behrens TE, Woolrich MW, Smith SM. Fsl. *Neuroimage*. 2012; 62(2):782–790.

657

658 Jenkinson M, Smith S. A global optimisation method for robust affine registration of brain images. *Medical image analysis*. 2001; 5(2):143–156.

659

660 Jungé JA, Scholl BJ, Chun MM. How is spatial context learning integrated over signal versus noise? A primacy effect in contextual cueing. *Visual cognition*. 2007; 15(1):1–11.

661

662 Kim H, Schlichting ML, Preston AR, Lewis-Peacock JA. Predictability changes what we remember in familiar temporal contexts. *Journal of cognitive neuroscience*. 2020; 32(1):124–140.

663

664 Kok P, Failing MF, de Lange FP. Prior expectations evoke stimulus templates in the primary visual cortex. *Journal of cognitive neuroscience*. 2014; 26(7):1546–1554.

665

666 Kok P, Mostert P, De Lange FP. Prior expectations induce prestimulus sensory templates. *Proceedings of the National Academy of Sciences*. 2017; 114(39):10473–10478.

667

668 Kok P, Turk-Browne NB. Associative prediction of visual shape in the hippocampus. *Journal of Neuroscience*. 2018; 38(31):6888–6899.

669 **Kuhl BA**, Rissman J, Wagner AD. Multi-voxel patterns of visual category representation during episodic encoding are
670 predictive of subsequent memory. *Neuropsychologia*. 2012; 50(4):458–469.

671 **Long NM**, Kuhl BA. Decoding the tradeoff between encoding and retrieval to predict memory for overlapping events.
672 *NeuroImage*. 2019; 201:116001.

673 **Long NM**, Kuhl BA. Cortical representations of visual stimuli shift locations with changes in memory states. *Current
674 Biology*. 2021; 31(5):1119–1126.

675 **Lu Q**, Hasson U, Norman KA. A neural network model of when to retrieve and encode episodic memories. *eLife*. 2022;
676 11:e74445.

677 **Oostenveld R**, Fries P, Maris E, Schoffelen JM. FieldTrip: open source software for advanced analysis of MEG, EEG, and
678 invasive electrophysiological data. *Computational intelligence and neuroscience*. 2011; 2011.

679 **Papademetris X**, Jackowski MP, Rajeevan N, DiStasio M, Okuda H, Constable RT, Staib LH. *BioImage Suite: An integrated
680 medical image analysis suite: An update*. *The insight journal*. 2006; 2006:209.

681 **Patil A**, Duncan K. Lingering cognitive states shape fundamental mnemonic abilities. *Psychological Science*. 2018;
682 29(1):45–55.

683 **Schacter DL**, Addis DR, Hassabis D, Martin VC, Spreng RN, Szpunar KK. The future of memory: remembering, imagining,
684 and the brain. *Neuron*. 2012; 76(4):677–694.

685 **Schapiro AC**, Kustner LV, Turk-Browne NB. Shaping of object representations in the human medial temporal lobe based
686 on temporal regularities. *Current biology*. 2012; 22(17):1622–1627.

687 **Schapiro AC**, Rogers TT, Cordova NI, Turk-Browne NB, Botvinick MM. Neural representations of events arise from tem-
688 poral community structure. *Nature neuroscience*. 2013; 16(4):486–492.

689 **Schapiro AC**, Turk-Browne NB, Botvinick MM, Norman KA. Complementary learning systems within the hippocampus:
690 a neural network modelling approach to reconciling episodic memory with statistical learning. *Philosophical Transac-
691 tions of the Royal Society B: Biological Sciences*. 2017; 372(1711):20160049.

692 **Schlichting ML**, Mumford JA, Preston AR. Learning-related representational changes reveal dissociable integration and
693 separation signatures in the hippocampus and prefrontal cortex. *Nature communications*. 2015; 6(1):1–10.

694 **Sherman BE**, Graves KN, Turk-Browne NB. The prevalence and importance of statistical learning in human cognition and
695 behavior. *Current opinion in behavioral sciences*. 2020; 32:15–20.

696 **Sherman BE**, Turk-Browne NB. Statistical prediction of the future impairs episodic encoding of the present. *Proceedings
697 of the National Academy of Sciences*. 2020; 117(37):22760–22770.

698 **Smith TA**, Hasinski AE, Sederberg PB. The context repetition effect: Predicted events are remembered better, even when
699 they don't happen. *Journal of Experimental Psychology: General*. 2013; 142(4):1298.

700 **Tanaka KZ**, Pevzner A, Hamidi AB, Nakazawa Y, Graham J, Wiltgen BJ. Cortical representations are reinstated by the
701 hippocampus during memory retrieval. *Neuron*. 2014; 84(2):347–354.

702 **Thavabalasingam S**, O'Neil EB, Zeng Z, Lee AC. Recognition memory is improved by a structured temporal framework
703 during encoding. *Frontiers in Psychology*. 2016; 6:2062.

704 **Tompry A**, Davachi L. Consolidation promotes the emergence of representational overlap in the hippocampus and
705 medial prefrontal cortex. *Neuron*. 2017; 96(1):228–241.

706 **Treder MS**, Charest I, Michelmann S, Martín-Buro MC, Roux F, Carceller-Benito F, Ugalde-Canitrot A, Rollings DT, Sawlani
707 V, Chelvarajah R, et al. The hippocampus as the switchboard between perception and memory. *Proceedings of the
708 National Academy of Sciences*. 2021; 118(50).